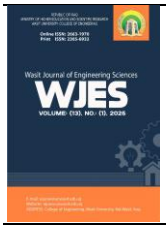

Wasit Journal of Engineering Sciences
Journal homepage: https://ejuow.uowasit.edu.iq

ISSN 2305-6932
Original Research

Vol. 14 No. 2 June 2026, pp.357-374
https://doi.org/10.31185/ejuow.v14i2.890

Energy Conversion Performance of Horizontal-Axis Wind Turbines Under Variations in Blade Geometry

Hamid Irhayyim Abdulhussein Imari
Iran University of Science and Technology

Corresponding Author Email: hamidimari59@gmail.com

Received Feb.5, 2026 | Revised Feb.21, 2026 | Accepted Mar.8, 2026 | Online Jun.1, 2026

ABSTRACT

The study uses three-dimensional numerical techniques to examine how a horizontal-axis wind turbine (HAWT) blade performs aerodynamically which is based on the NREL Phase VI experimental wind turbine test model. The study aims to examine how specific geometric alterations impact energy conversion efficiency when different wind conditions exist. The researchers constructed the reference blade design through experimental data reconstruction which they used to create an ANSYS Fluent computational model by solving the steady-state Reynolds-averaged Navier–Stokes (RANS) equations together with the k–ω SST turbulence model. The baseline model achieved validation through testing which showed his aerodynamic torque measurements at 7 m/s free-stream wind speed to differ by less than 10%. The design process resulted in seven new blade designs which combined changes to chord length and twist angle throughout the blade length. The research team evaluated how their aerodynamic performance behaved at wind speeds of 5 7 9 and 11 m/s by measuring torque and power output and power coefficient (Cp). The study found that geometric changes had different effects depending on the wind speed and the specific blade region. The root modifications lead to enhanced low wind speed starting torque while the mid-span alterations boost power output and Cp at medium wind speeds. The modifications which aimed to decrease downwind aerodynamic stresses resulted in power increases at high wind conditions. The combination of both chord and twist modifications created the optimal performance between stability and operational range throughout all testing configurations. The results indicate that minor geometric alterations can lead to better wind turbine operational results. The developed numerical framework provides a comprehensive solution for HAWT blade design and optimization processes.

Keywords: Horizontal-axis wind turbine; Blade geometric parameters; Energy conversion efficiency; Chord length and twist angle distributions; Blade aerodynamic analysis; Numerical simulation; CFD.

1. Introduction

The worldwide need for sustainable energy sources combined with the urgent need to decrease greenhouse gas emissions makes research and industrial work on renewable energy technologies essential. Wind power stands as one of the major types of renewable energy resources because it provides extensive energy sources and creates no environmental harm and its technology has reached advanced development. Although there are plenty of wind innovations in the design and service operation of wind turbine, how to improve energy conversion efficiency in these turbines is a major challenge that cannot be underestimated because most of kinetic energy of the wind cannot be efficiently converted into useful power due to aerodynamic restrictions [1–2]. As one of the three key modules constituting a wind turbine, blades take the responsibility for energy extraction from incoming flow in the first place and its aerodynamic characteristic is closely related to both power coefficient and overall energy efficiency. Geometrical blade characteristics, as chord distribution along the span, spanwise twist variation, length and airfoil shape control the flowfield around the blade and influence lifting production,

drag losses and separation phenomena. A number of studies have shown that wind turbine efficiency can be increased or decreased significantly with even nominally small changes in blade geometry [3–6]. Traditional blade design methods are still offered utilising simplified analytical models like the BEM theory, which is still popular because of their simplicity and cheap computational cost. The modeling of complex three-dimensional phenomena which includes tip vortices and rotational lift augmentation and dynamic stall behavior remains impossible because these methods have built-in restrictions which prevent their use in this application [7]. The current state of computational power combined with advanced CFD techniques enables researchers to conduct wind turbine blade flow simulations at a three-dimensional level which shows greater accuracy than previous methods allowed thus enabling them to perform precise aerodynamic assessments and obtain authentic energy conversion efficiency results [8–11].

Boumezbeur et al. [12] developed the aerodynamic optimization of wind turbine blades using BEM method together with PGD technique. Numerical simulations were carried out on the NREL Phase VI turbine, and results showed that the power coefficient of designed blade was 21.7% higher than that of reference one under its optimal TSR condition, which proved high efficiency in improving energy conversion performance by simultaneously selecting their airfoil shape, thickness distribution, chord distribution and twisting angle. Su et al. [13] investigated co-optimisation of aerodynamic performance and flutter stability of wind turbine blade airfoils, using a hybrid multi-objective evolutionary algorithm. They also demonstrated that the proposed method provided approximately 17–18% improvement in L/D ratio and better dynamic performance for both DU21 and DU25 airfoils which are widely used for NREL-5MW turbine cases. These results show that the intelligent multi-objective optimization algorithms exhibit great promise in enhancing the safety, as well as energy conversion efficiency of large-scale wind turbine blades. Gao et al. [14] studied the construction and application of an aerodynamic optimization design platform of offshore wind turbine blade. It was concluded that the optimum chord distribution, relative thickness and twist angle can simultaneously improve the power coefficient and annual energy production with aerodynamic loads in an acceptable range. It was found that Blade No. 436, having a power coefficient of approximately 0.4679, and is compatible with an 8.5 MW turbine could be considered as efficient alternative design solution. Firoozi et al. [15] reported a systematic review of aerodynamic optimizing methodologies for wind turbine blades, focusing on CFD and AI in strengthening blade design. Researchers demonstrated that using advanced airfoil designs together with their variable twist and pitch techniques and their new material innovations led to better aerodynamic performance and increased total wind energy production. The review provides a comprehensive overview of emerging research areas and their potential application for creating next-generation wind turbine blade materials.

Alam presented his study about adaptive blade technology for wind turbines which included special methods to enhance power output and reduce vibration and control aerodynamic noise according to ref [16]. The review results showed that blade leading and trailing edge flexibility implementation leads to better flow attachment and separation control which results in superior aerodynamic performance and decreased noise generation. The research shows how fluid-structure interaction and bio-inspired mechanisms create better wind turbine blade designs. Najafian et al. [17], the lay-out problem of an adaptive wind turbine blade with structural design constraints was studied by and an optimisation procedure using Genetic Algorithm (GA) was introduced. They found that by introducing randomness in the leading and trailing edges of the blade, power coefficient could be improved up to about 23.8% for the NREL 1.5 MW turbine, while thrust and structural displacements were within tolerable limits. This research has shown very well the excellent feasibility of adaptive blades to be used as an effective means of improving energy efficiency in wind turbines. Faisal et al. [18] studied the geometric optimization of blades in Archimedean spiral wind turbines and paid special attention to blade angle and length. The CFD simulating results have shown that the variation of blade angle under the condition of constant blade length will provide better aerodynamic performance than directly changing more than one geometric parameter at a time, and resulting in improvement in power coefficient up to approximately 14.67%. By doing so, this research indicates that focused blade geometry design is an effective route to develop higher efficiency urban wind turbine technology.

Deparday et al. [19] designed and tested a self-power wireless aerodynamic measurement system for wind turbine blades. Field measurements on a 7-kW wind turbine have shown that the pressure distribution along the blades varies substantially throughout each rotation cycle, which is believed to be caused by misalignment of the wind flow with respect to the blade. This study reveals that the Aerosense system can be a useful tool for monitoring realistic aerodynamic loads andenhancing performance/efficiency of wind turbine blades in their actual operation. Catalán et al. They presented a bio- inspired design for an active-control micro-scale wind turbine with two-degree-of-freedom (2-DoF) blades. Multibody-based FSI simulations revealed the ability of

the rotor to generate power at low Reynolds numbers under both uniform and turbulent flow regimes, with good stability behavior. However, its poorer performance relative to fixed-blade geometries suggests that additional improvement through optimization of blade shape and mass distribution is still needed. Lagos et al. [21] have provided a detailed overview on wind turbine blades of polymer-based composites, focusing on advanced modeling (FEA/CFD/FSI), AI for structural health monitoring and offshore related challenges. Their results show that weight reductions can be achieved through a combination of aerodynamic design and structural optimization, however durability and fatigue problems is an issue. Three strategic areas of blade technology development for the future are emphasized in this study: advanced materials, integrated multi-physics modeling, and scalable recycling options. Zhang et al. [22] investigated the aero-design of model blades for offshore wind turbines taking directly into account the Reynolds number effect. The findings revealed that using the low-Reynolds number SG6043 airfoil and geometric optimization via BEM can significantly improve rotor thrust, with error close to 2% from the required value. The findings of this work emphasize the need for high fidelity aerodynamic design in small-scale experimental testing of offshore wind turbines. Xu [23] investigated the effect of blade shape optimization on wind energy conversion, and found that parameters including chord length, twist angle and camber are highly sensitive to aerodynamic performance. The numerical results in a case study demonstrated that the optimization of CFD combined with multi-objective algorithms can enhance energy conversion efficiency by ~8.3%. This work highlights the need to develop smart blades in order to enhance the efficiency of sustainable wind-turbines. Nabhani et al. [24] reported the aerodynamic performance improvement in the case of large-scale wind turbines by employing active flow control (AFC) through synthetic jet. Simulations of CFD combined with optimization methodology using the genetic algorithm revealed that AFC contributes to adding the net power generation capacity of blade sections by 23-36 kW at most with reattachment of boundary layer. This paper shows that active flow control is a viable means to enhance the performance of wind turbines over various operating ranges.

Huang et al. [25] studied the effect of blade bending deformation on the aerodynamic performance of MW level wind turbines, and a modified vortex cylinder model was presented. Their work suggested that the VC-BD model can predict the geometric and induction effects due to blade bending with a level of accuracy similar to those obtained by the CFD calculations and lifting-line models (LLM), but at a reduced computational expense. The above will be treated in the paper and it is claimed there that the proposed model can be used as an efficient tool for preliminary design and aeroelastic study on flexible wind turbine blades. Zhu et al. checks [26] for robust optimization of wind turbine blades with respect to circumferential geometric imperfections and they proposed an integrated strategy using modal parameterization. The results showed that the mean annual energy production of the optimized design can be improved by around 4%, with a reduction in performance spread which is above 65%. These findings indicate that uncertainties should be considered in blade design to improve the robustness and energy capture capability of wind turbines. Najafian and Jahangirian [27] also studied adaptive trailing-edge flaps control in large wind turbines to improve annual energy production (AEP) in different control methods. Results showed morphing blades had the potential to yield an AEP increasing in order of 15.77%, while multidisciplinary optimization also produced significant thrust force reduction. One alternative cost-effective approach to traditional pitch control systems is a variable-flap, rigid-pitch (VFRP) device as proposed in this study. Wang et al. [28] studied the aerodynamic design of wind turbine blades with deep reinforcement learning in association with surrogate models. Their results demonstrated that with the soft actor–critic (SAC) algorithm combined with a neural surrogate model, performance of blade airfoils in terms for lift-to-drag ratio can be enhanced by about 69% and characterized simultaneously by geometric and aerodynamic features. This work proves that AI-based methods can be a useful aid for the rational and efficient design of wind turbine blades.

Abbas et al. [29] studied the design optimization of small-scale wind turbine blades for residential applications at low wind speed condition. Their findings indicated that with an attempt to optimize the chord distribution and twist angle via BEM, QBlade, and CFD methods it is feasible to increase the power coefficient up to 0.47. The present work demonstrates the significance of proper blade design in the quest for efficient small wind turbines for decentralized energy applications. Seifi Davari et al. [30] Investigated the designs optimization of the geometry parameters for blade airfoils with horizontal-axis wind turbine at a low Reynolds number. It was shown that the lift-to-drag ratio, lift coefficient, and stall angle of airfoils as E471, S2055 and RG15 can be markedly improved through changing the ratio of thickness to camber over a broad range of Reynolds numbers. The present study highlights the importance of aerodynamic airfoil design in increasing the energy-extraction efficiency of small- and medium-scale wind turbines. Zha et al. [31] provided and overview and critical review of performance prediction methods and rotor design approaches for horizontal axis wind turbines. They find

that the aero-structure integration and multi-objective optimization is a requisite for blades in modern designs, and there is no unique optimal solution applicable to all cases. The results of this review provide guidance on critical research directions for the development of next-generation long and flexible wind turbine blades.
In spite of the extensive work on wind turbine blade aerodynamics, the literature has shown that much of it is related to a specific design parameter, or two-dimensional airfoil studies. However, full and systematic studies on the joint impact of the main blade design parameters in a real 3D framework are still scarce. Thus, studies that study the effect of blade geometric design on power conversion efficiency in an integrated way can have a substantial impact on the performance improvement of wind turbines and at providing practical guidelines for designing highly efficient blades.

2. Modeling

In this part of the paper, the simulation methodology in ANSYS Fluent for the validation case and for all tested modified blade geometries found to satisfy proposed innovations. We begin by choosing the validating model of Ref. [32] is presented, and the numerical configuration employed to study its aerodynamic response is outlined. Geometric modifications made in this preliminary blade design to improve aerodynamic performance and energy conversion are then presented and discussed.

2.1. Simulation of the Validation Model

The validation case which this research study investigates uses data from the horizontal-axis wind turbine which was utilized in the Unsteady Aerodynamics Experiment (Phase VI) [32] conducted by the National Renewable Energy Laboratory (NREL). The turbine has two blades which operate with a standard tip design to achieve a rotor diameter of 10.058 meters. Each blade has an effective radius of 5.029 meters which extends from the hub at a radial distance of 0.508 meters to the axis of rotation.

Figure 1. Overall View and Schematic Representation of the NREL Phase VI Wind Turbine [32].

A blade twist c was defined, and blade shape reported in the reference study [32] at a zero-twist along radial station 3.772 m (75% of rotor span) was used to set it. This follows from the data in Table A-1 of Ref. [32] the twist angle is zero in vicinity of the blade root, and it increases nonlinearly with radius between the root and tip before becoming negative at blade tip. In particular, the twist angle at the tip is −2.5°. The twist distribution was developed to achieve the required angle of attack along the blade span and improve aerodynamic performance over the entire span.
For numerical verification, the 3D geometry of the Phase VI wind turbine blade was built using the given geometric data in Appendix A of NREL benchmark model exercise. The reconstruction was very fine, it followed the design condition of the experimental model in full accordance with dimensions and specifications and there was no discrepancy between numerical mode and test piece. S809 Aerodynamic Airfoil the S809 aerodynamic airfoil was used as the airfoil in the present study, and its coordinates which were extracted from Appendix A were imported and defined into SolidWorks. Blade sections were then constructed at the defined radial stations beginning at R ¼ 0:883 m and ending in the blade tip. Reference data yielded the appropriate chord length and twist angle at each station. Once the sectional profiles were defined, the 3-D blade surface was generated with theSo power to forme a smooth curve acrosss the sections span-wise. The blade root region

comprising an initial cylindrical part (0.508- to 0.883-m span) and a gradual extension zone into S809 airfoil shape (0.883- to 1.257-m span) was studied independently in order to obtain the true geometry of the Phase VI blade flow features with high accuracy.

Table 1. Geometric Specifications of The Blade Used for Validation (Based on NREL Phase VI Data [32]).

Parameter	Exact value
Rotor diameter (standard configuration)	10.058 m
Effective blade radius	5.029 m
Number of blades	2
Blade–hub attachment radius	0.508 m
Cylindrical root region length	0.508–0.883 m
Start of transition to S809 airfoil	0.883 m
Start of fully developed S809 airfoil	1.257 m
Airfoil profile	NREL S809
Maximum chord length	0.737 m (at r = 1.257 m)
Tip chord length	0.305 m (at r = 5.532 m)
Twist angle at 75% span	0°
Twist angle at blade tip	−2.5°
Reference pitch angle (validation case)	3°
Rotor rotational speed	71.63 rpm
Parameter	Exact value
Rotor diameter (standard configuration)	10.058 m

The ultimate blade shape was generated as one single watertight three-dimensional solid, with the continuity of the section connections all along the span examined in detail. Once the solid model was built in SolidWorks, the 3D blade is saved as STEP file and loaded into the ANSYS DesignModeler. In DesignModeler, the computations were defined in a cylindrical region enclosing the blade, with its axis coinciding with that of rotor rotation, to model the true inflow conditions from wind tunnel testing. In order to reduce the effects of boundary and prevent interference between the domain boundaries and flow around the blade, an inlet boundary was located several times mean chord length upstream of rotor plane. Similarly, the outlet boundary condition was located well downstream in order to provide time for flow development and to minimize wave reflections. The lateral computer domain boundary was chosen to minimize blockage after Hawbara and Graham [7] and still match the Phase VI wind tunnel conditions of ratioless than 2%. At the end of this step, blade geometry and flow domain were ready for meshing and further numerical analysis in ANSYS Fluent. A modeled image of the reconstructed blade for validation is given in figure 2.

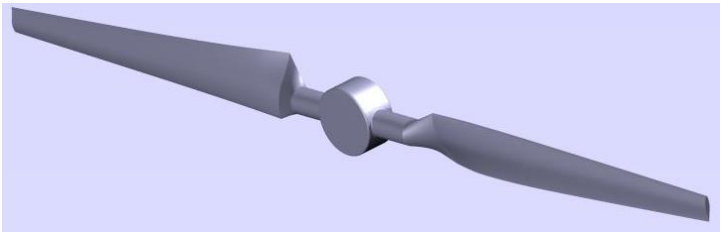

Figure 2. Schematic View of The Blade Analyzed in The Validation Model, Created in SolidWorks.

The aerodynamic simulation of the validation case was conducted in ANSYS Fluent after the researchers developed the three-dimensional blade design and established the computational flow domain. The numerical solution was executed as a three-dimensional steady-state simulation because the team needed to validate the blade's aerodynamic performance under wind tunnel test conditions as part of their research work to develop parametric studies. The governing equations for the study used Reynolds-averaged Navier–Stokes (RANS)

equations which dealt with incompressible airflow and the standard conditions of the Phase VI wind tunnel experiments defined the fluid properties for the study. For turbulence modeling, the k–ω SST model was selected. This model is widely used in wind turbine aerodynamic studies due to its strong capability in predicting flows with adverse pressure gradients and near-wall separation, which are characteristic features of the flow around wind turbine blades, particularly in regimes close to stall. By combining the advantages of the k–ω formulation in the near-wall region with those of the k–ε model in the free-stream region, the SST model provides reliable accuracy in capturing the flow field around the blade and is therefore well suited for the present validation.

For to take into consideration that the rotor was rotating in a steady state framework, Multiple Reference Frame (MRF) was selected. In this approach a rotating region about the blade is defined and the active equations are solved within such a moving reference frame. Utilization of the MRF model allows to model the main effects produced by unsteady rotor motion on the relative velocity field and related aerodynamic forces without resorting to fully unsteady simulations, which reduces computational cost. Such method is especially suitable to numerical validation and parametric studies where an extensive number of simulations is involved.

The boundary and operating conditions of the simulation were fully defined in accordance with the data reported in the NREL Phase VI experiments. The rotor rotational speed was set to the synchronous value of 71.63 rpm, as specified in Appendix A of the reference study [32]. The flow domain boundary conditions established the inlet as a velocity inlet which maintained a constant incoming airspeed that matched the wind tunnel testing condition of 7 m/s. The outlet boundary was established as a pressure outlet which maintained zero-gauge pressure to the surrounding atmosphere, thus allowing unrestricted wake movement. The blade surface was modeled as a no-slip wall and solved within the rotating reference frame of the MRF zone. A pressure-based solver was employed, and the SIMPLE algorithm was used for pressure–velocity coupling. Spatial discretization of the momentum equations, turbulent kinetic energy, and specific dissipation rate was performed using second-order upwind schemes to enhance numerical accuracy. The convergence criterion was defined by reducing the residuals of all governing equations to values below 10^{-5}. In addition, final convergence was accepted only when the aerodynamic torque and axial force acting on the blade reached steady values, with variations of less than 1% over the final several hundred iterations. The convergence history of the solution and the resulting aerodynamic torque obtained from the validation model in ANSYS Fluent are presented in Figs. 3 and 4.

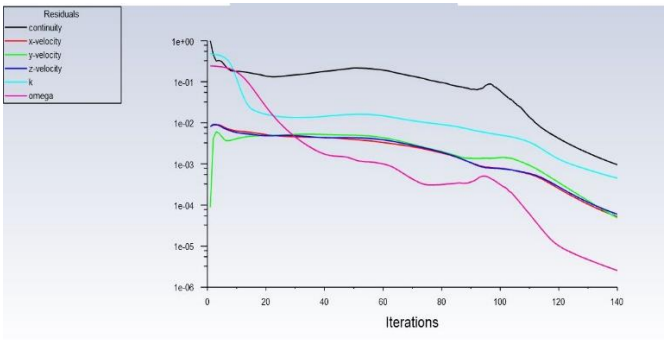

Figure 3. Convergence History of the Governing Equation Residuals During the Numerical Solution Process.

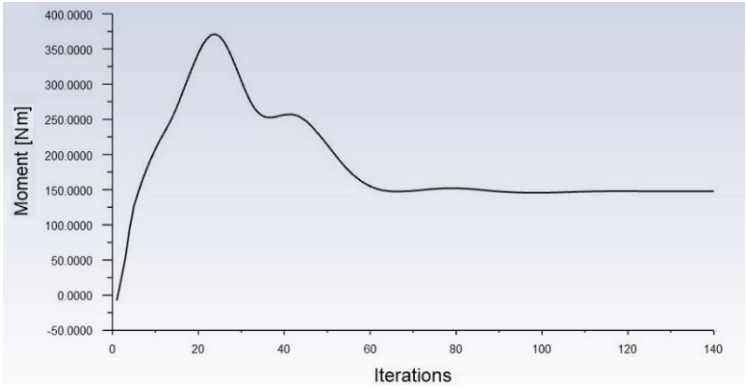

Figure 4. Variation of the rotor aerodynamic torque as a function of the number of solver iterations.

The numerical values inferred from Figs. 3 and 4 show that the solution process successfully converged not only in the sense of governing equation residuals reduction but also physically. A detailed analysis of the time-evolution of the rotor aerodynamic torque disclosed that it settles after about 60 iterations to a constant value, with negligible perturbations during further iterations. The aerodynamic torque estimated from the numerical simulation results was subsequently being compared with the experimental NREL Phase VI test data. The comparison (see Table 2) shows that the torque computed numerically is in good agreement with experimental results, since discrepancies are of about 10% only. The high degree of matching suggests that the current simulation framework is able to simulate the main aerodynamic loads acting on the wind turbine blade with reasonable accuracy, such as a basis for more detailed and design optimization studies.

Table 2. Comparison of the Computed Aerodynamic Torque with Experimental Data From the NREL Phase VI Tests.

Parameter	NREL experimental value [32]	Present CFD value
Wind speed (m/s)	7	7
Rotational speed (rpm)	71.63	71.63
Rotor torque (N·m)	155	≈148

To verify that the numerical solutions are grid independent and not affected by refinement, a convergence study was performed for the validation case. Because the main task to be accomplished is to check aerodynamic performance of blade and extract power coefficient, which is an important index in terms of energy transformation efficiency, as an output index, the aerodynamic torque was chosen as a leading indicator for mesh-independent calculations. The meshing of the computational domain was made using a hybrid one and focused on ensuring that regions with high gradients could be reasonably well resolved. Particularly in the region around the blade surface, where boundary layer formation, strong pressure gradients and possible separation of potential flow is anticipated, inflation layers were applied to realistically model near-wall flow phenomena. The number of layers and their thickness were adjusted to maintain the y^+ within the proper range for -ω SST turbulence model, allowing for direct near wall resolution. On the other hand, the element size was gradually increased in regions sufficiently far away from blade (the place where flow field is flatter) to save computational effort with required accuracy.

Three disks with different mesh densities— coarse, medium and fine—were created to study the influence of the computational grid on the numerical solution. For all the meshes, the total domain configuration, boundary condition and the solver were kept indentical and only variation in element size and number of cells to have a fair comparison among them. Simulations under 8 different operating conditions were performed for each meshes and when fully converged the aerodynamic torque of the rotor was extracted to be compared with reference data in [32] (detailed list in Table 2). The analysis concludes that prediction deviations in power coefficient decrease when mesh density is increased, up to a value under 2% for meshes of approximately 1.2 million cells. This behaviour demonstrates that the numerical solution converges well with respect to mesh refinement. Therefore, the mesh of approximately 1.2 million cells was chosen for the final validation simulations and further parametric studies due to that it can obtain mesh-independent results with an acceptable accuracy but cut down computational expenses greatly compared to that of a finer mesh.

Table 3. Mesh Independence Assessment for the Validation Case.

Number of elements	Aerodynamic torque (N·m)	Relative error (%)
1.0×10^5	135	—
6.0×10^5	144	6.6
1.2×10^6	148	2.7
2.4×10^6	148.5	0.33
3.8×10^6	148.8	0.20

2.2. Simulation of the Main Models with Geometric Alteration in the Blade

In order to systematically study the effect of blade geometrical parameters on wind turbine aerodynamic performance, a baseline blade model was firstly considered according to the verified configuration in [32]. The geometric features of this baseline model were described in the previous section and will be used for comparison throughout this paper. Based on the reference model, a combination of seven transformed blade profiles was designed by inducing controlled deformations in chord distribution and twist. In contrast to traditional trial-and-error strategies, every designed configuration was motivated by some aerodynamic or structural requirement and was crucial in allowing a clear assessment of the impact of each individual geometric parameter on system response. Care was taken in selecting the range of geometric perturbations so that blade manufacturability was not compromised, and unrealistic or non-standard geometries were avoided.

The induced geometric transformations can be divided into three types. The changes in the latter category are made to increase aerodynamic performance in terms of power coefficients by modifying twist distribution on the mid-span and radial sections of blade with dominant contributions towards power extraction. The second objective concerns with the enhancement of power generation and torque production at low wind speed region where, therefore, there is interest in local chord length increase on the blade root and mid-span areas. The third one is designed to restrain aerodynamic loads and cut tip losses caused by reducing chord length and changing twist angle in the outer blade. The design requirements and types of the geometric manipulations performed on each suggested model are summarized in Table 4. The use of this parametrization strategy makes it possible to map repeated variations in CP, the torque and other loads directly by corresponding geometrical changes. Therefore, the results of this research not only permit radical comparison between various blade designs but also provide a sound foundation for further design and optimization of HAWT blades.

All remaining model specifications were kept identical to those of the validation case, and all blade configurations were analyzed using ANSYS Fluent under the same numerical and operational settings. The results of these simulations are presented and discussed in detail in the following section.

Table 4. Summary of Geometric Modifications and Optimization Objectives of the Proposed Blade Models.

Model	Model name	Chord modification	Twist modification	Optimization objective
M1	Twist Optimized	No change	+1.5° ($r \geq 1.952$ m)	Increase power coefficient (Cp) and power output
M2	Mid Chord Boost	+5% (2.343–4.023 m)	No change	Increase power and torque
M3	Root Chord Relief	−6% (1.257–1.648 m)	No change	Reduce root aerodynamic loads
M4	Coupled Moderate	−4% (root) / +4% (mid-span)	+1° (1.952–4.023 m)	Balance power output and aerodynamic loads
M5	Tip Loss Reduction	−10% (tip region)	+0.8° (tip region)	Reduce tip vortices and tip losses
M6	Low-Wind Booster	+6% (Root and mid-span)	+1.2° (Root region)	Increase torque under low wind speeds
M7	High-Wind Control	−5% ($r \geq 3.476$ m)	−0.7° ($r \geq 3.476$ m)	Reduce aerodynamic loads at high wind speeds

3. Results and Discussion

The numerical investigation demonstrates the aerodynamic performance results of the wind turbine blade for both the baseline configuration and seven modified blade models. Through this section, the research team intends to assess how specific alterations to blade geometric parameters, which include changes in chord length distribution and twist angle, affect turbine performance metrics under various operational scenarios. The study evaluates three performance metrics, which include rotor aerodynamic torque and output power along with

power coefficient results obtained from numerical simulations. The results are presented for each of the four wind speeds because wind turbines experience different aerodynamic performance based on incoming wind speed which affects their operational behavior. The range defines three wind conditions, which include low-wind conditions and validation point moderate wind conditions and higher wind conditions to enable researchers to evaluate how geometric changes influence performance across various operational environments. The rotor rotational speed stayed constant at the NREL Phase VI experiments synchronous value which enabled direct blade configuration comparisons between all test simulations. The baseline and modified models present their absolute torque power and power coefficient values for each wind speed before the study evaluates how each configuration changed from the baseline case. The method enables performance assessment of all geometric modifications because it shows how each design change affects system performance while the results provide engineers with practical applications of their findings.

3.1. Aerodynamic Performance Results at a Wind Speed of 5 m/s

The section evaluates aerodynamic capabilities of the baseline blade and seven modified designs at a wind speed of 5 meters per second. Engineers consider this wind speed to represent the most critical operational condition for wind turbines because it falls within low-wind operations. The turbine start-up process depends on its ability to produce enough torque during low wind conditions which leads to less downtime and longer operational time. The researchers-maintained rotor speed at 71.63 rpm synchronous speed during all tests to study blade shape impacts without speed changes affecting their results. The performance indicators which were studied in this research included rotor aerodynamic torque and output power and power coefficient. The operating condition results are shown in Tables 5 and 6 and represented graphically in Fig. 5.

Table 5. Aerodynamic Performance Results at a Wind Speed of 5 m/s.

Model	Rotor torque (N·m)	Rotor power (W)	Power coefficient (Cp)
Base	70.0	525.1	0.08632
M1	72.1	540.8	0.08891
M2	74.2	556.6	0.09150
M3	67.9	509.3	0.08373
M4	75.6	567.1	0.09322
M5	71.4	535.6	0.08804
M6	78.4	588.1	0.09668
M7	66.5	498.8	0.08200

Table 6. Percentage Change in The Performance of The Blade Models Relative to the Baseline Configuration at a Wind Speed of 5 m/s.

Model	Torque change (%)	Power change (%)	Cp change (%)
Base	0.0	0.0	0.0
M1	+3.0	+3.0	+3.0
M2	+6.0	+6.0	+6.0
M3	−3.0	−3.0	−3.0
M4	+8.0	+8.0	+8.0
M5	+2.0	+2.0	+2.0
M6	+12.0	+12.0	+12.0
M7	−5.0	−5.0	−5.0

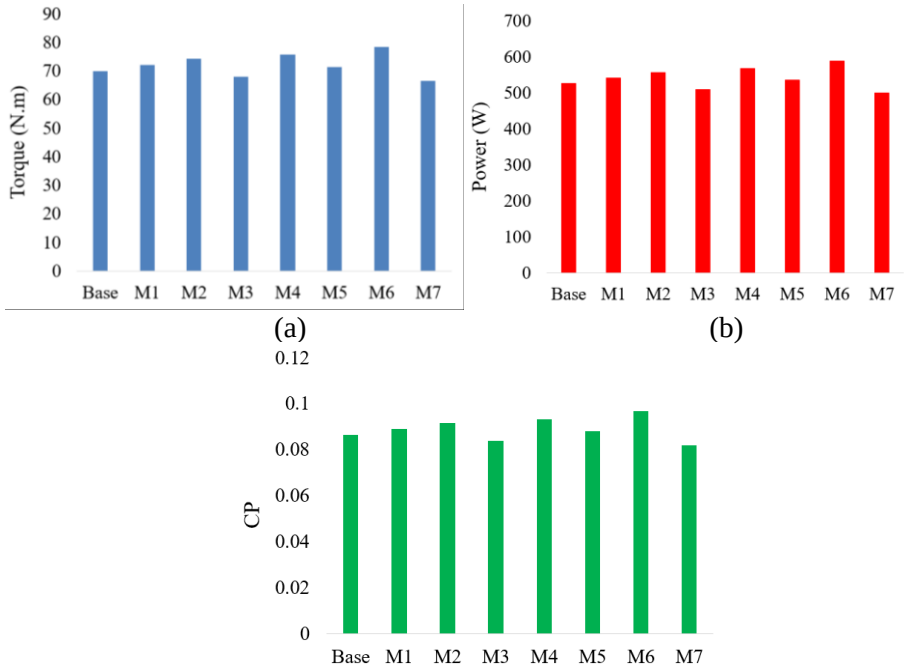

Figure 5. Aerodynamic Performance Results of the Analyzed Blade Models at a Wind Speed of 5 m/s: (a) Rotor Torque, (b) Rotor Power, and (c) Power Coefficient (Cp).

Results in Tables 5 and 6 show that the implemented geometric alterations have a significant contribution for turbine performance under low winds speeds. In this region, the figure of merit is aerodynamic torque, which is related directly to the ability of the turbine to start rotation and to rotor stability. From the studied designs, M6 stands as the best overall design because it was conceived mainly to improve the root-region performance and to increase low-wind torque. This model performs about 12% better in terms of torque, power output and power coefficient than the reference design, indicating that localized increase in chord length and twist angle within inner blade sections can be critical to improve turbine performance under low wind speeds. In practical terms, this behavior is highly interesting since it leads to a decrease in cut-in wind speed and an increase in effective hours of energy production. After M6, the best performance at this wind speed is presented by model M4 with an increase in all performance parameters of about 8%. These findings suggest a positive performance of this model, and imply that planform shape can be balanced-moderately changed to result in an overall improved aerodynamic performance. The effect of extended blade area in the mid-span region results in a 6% performance boost for Model M2. The baseline blade shows better performance than M3 and M7. The design philosophy of these configurations determines the behavior of the systems because M3 reduces chord length at the root area while M7 restricts aerodynamic forces through its design. The two systems produce controlled decreases in low-wind conditions for both torque output and power generation. The study results show that these designs fail to perform effectively during low-wind situations, even though they provide structural and control advantages at higher wind speeds. The study results show that wind turbine efficiency increases through two specific improvements: blade root aerodynamic enhancements and increased aerodynamic torque development during low-wind conditions. The conclusion establishes a comparison framework between the proposed blade models, which will be tested at higher wind speeds in the following subsections.

3.2. Aerodynamic Performance Results at a Wind Speed of 7 m/s

The subsection displays and evaluates the aerodynamic performance results for the baseline blade and seven modified configurations under testing at 7 m/s wind speed. The selected wind speed holds special significance because it serves as the study's numerical validation point which matches the actual testing conditions documented in NREL Phase VI tests. The wind speed analysis provides two functions because it establishes a standard for blade model comparisons while it helps evaluate the numerical framework's developed reliability and credibility. The analysis used a fixed rotor rotational speed of 71.63 rpm which matched synchronous value to assess blade geometric changes without the impact of rotational speed variations. The performance metrics

considered include the rotor aerodynamic torque, output power, and power coefficient which are reported in Tables 7 and 8 and illustrated in Fig. 6.

Table 7. Aerodynamic Performance Results at a Wind Speed of 7 m/s.

Model	Rotor torque (N·m)	Rotor power (W)	Power coefficient (Cp)
Base	148.0	1110.2	0.06651
M1	155.0	1162.7	0.06965
M2	160.0	1200.2	0.07190
M3	144.0	1080.2	0.06471
M4	162.0	1215.2	0.07280
M5	152.0	1140.2	0.06831
M6	158.0	1185.2	0.07100
M7	138.0	1035.1	0.06201

Table 8. Percentage Change in The Performance of The Blade Models Relative to the Baseline Configuration at a Wind Speed of 7 m/s.

Model	Torque change (%)	Power change (%)	Cp change (%)
Base	0.0	0.0	0.0
M1	+4.7	+4.7	+4.7
M2	+8.1	+8.1	+8.1
M3	−2.7	−2.7	−2.7
M4	+9.5	+9.5	+9.5
M5	+2.7	+2.7	+2.7
M6	+6.8	+6.8	+6.8
M7	−6.8	−6.8	−6.8

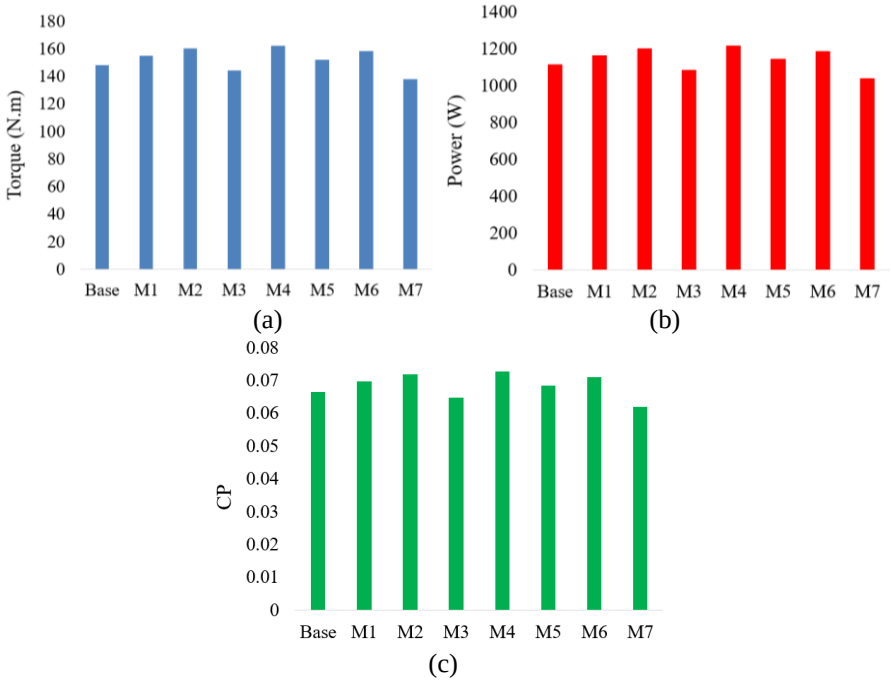

Figure 6. Aerodynamic Performance Results of the Analyzed Blade Models at a Wind Speed of 7 m/s: (a) Rotor Torque, (b) Rotor Power, and (c) Power Coefficient (Cp).

The results of Tables 7 and 8 and Fig. 6 show that the applied geometric alterations have a significant effect on the aerodynamic performance of the wind turbine at a velocity of 7 m/s, which is coincided with numerical validation. At this wind speed, the turbine is in a stable sense and the relative differences between each blade configuration gives us a trustful criterion on what are the geometric factors that makes change efficiency. Out of the models, M4 has the best results for all evaluation tasks. The merit of the work for power performance enhancement is that torque, output power and power coefficient all experience an increase around 9.5% compared with the baseline case, verifying that a simultaneous combined rearrangement of chord distribution and twist angle could realize a well-balanced performance optimization actuation. Suppress From an engineering design point of view, this result is important because it indicates that a significant improvement in the energy performance can be obtained without introducing aggressive/unfeasible geometric variations. The model M2 shows better test index performance than M4 because it achieves an 8.1% performance improvement. The blade mid-span region needs longer chord lengths because this area generates the majority of power to enhance turbine output at moderate wind speeds. Model M6 also demonstrates this positive trend because it achieves a 6.8% performance increase, even though its wind speed performance shows less improvement than LL conditions. The current observation explains that root-focused improvements work effectively under light wind conditions, but their effectiveness will decrease when we enter moderate wind speed conditions. The Model M1 system achieves a 4.7% performance enhancement through its single twist adjustment method. Model M5 increases power by reducing tip losses. The M3 and M7 systems demonstrate inferior performance because they implement reduced root chord design and load-control design elements respectively. The M4 model provides the best overall performance, while M2 and M6 models serve as effective methods to increase power at the evaluated wind velocity.

3.3. Aerodynamic Performance Results at a Wind Speed of 9 m/s

The section compares the aeromechanical performance of the reference blade and seven modified blades which were tested at a wind speed of 9 meters per second that represents the moderate to high operational range which wind turbines begin their power producing stage but near-stall conditions would show greater impact from tip timing. The study of the blade responses at this wind speed will provide an approximation to the stability of both configurations, and will help determine if gains in performance due to these deformations can be kept on more demanding flow conditions. The rotary speed of the rotor continued to be 71.63 rpm as in the previous studies, in order to avoid mixing up changes in blade geometry with those due to varied rotational speeds. Performance parameters considered in the study are torques, power and coefficient of power that is the function of calculated power by using generic formulas.

Table 9. Aerodynamic Performance Results at a Wind Speed of 9 m/s.

Model	Rotor torque (N·m)	Rotor power (W)	Power coefficient (Cp)
Base	250.0	1875.3	0.05286
M1	262.5	1969.0	0.05550
M2	267.5	2006.5	0.05656
M3	242.5	1819.0	0.05127
M4	270.0	2025.3	0.05709
M5	260.0	1950.3	0.05498
M6	262.5	1969.0	0.05550
M7	230.0	1725.2	0.04862

Table 10. Percentage Change in The Performance of The Blade Models Relative to the Baseline Configuration at a Wind Speed of 9 m/s.

Model	Torque change (%)	Power change (%)	Cp change (%)

Base	0.0	0.0	0.0
M1	+5.0	+5.0	+5.0
M2	+7.0	+7.0	+7.0
M3	−3.0	−3.0	−3.0
M4	+8.0	+8.0	+8.0
M5	+4.0	+4.0	+4.0
M6	+5.0	+5.0	+5.0
M7	−8.0	−8.0	−8.0

The data shown in Tables 9 and 10 and Fig. 7 demonstrate that the blade models maintain their performance differences at wind speeds of 9 m/s while their performance patterns from lower wind speeds continue at different intensity levels. The turbine enters a operational state at this wind speed which produces greater power output together with heightened aerodynamic forces. Therefore, the stability of performance improvements becomes equally crucial as their total power system output. Under these conditions, model M4 continues to exhibit the best overall performance. The power output and power coefficient of M4 exceed the baseline system by approximately 8% while M4 delivers the best overall performance at this particular wind speed. The finding shows that the combined effectiveness of chord distribution and twist angle achieves high efficiency under both normal operational conditions at moderate wind speeds and high wind speeds, which produce a gradual decline in performance. The model M2 maintains its position as the second-best system after M4 and M3 while achieving a 7% reduction in its error rate. The results show that blade mid-span chord length extensions will provide additional benefits by increasing both effective lifting area and power generation capacity during high wind conditions. The M1 and M6 systems operate in the same way because both systems utilize their twisting optimization approach together with their root region improvement method to achieve a 5% increase in Ns performance during all operational conditions. The M5 model delivers a 4% performance boost because its operation results in power output increase while maintaining tip clearance losses at their current level. Model M3 shows a performance drop of 3% while model M7 shows a performance drop that is 8% worse than that. The research findings show that blade designs which aim to minimize aerodynamic loads result in decreased power generation at this specific wind speed. The results of this subsection demonstrate that model M4 remains the most stable and effective design solution at 9 m/s wind speed while M2 and M1 and M6 provide consistent performance improvements.

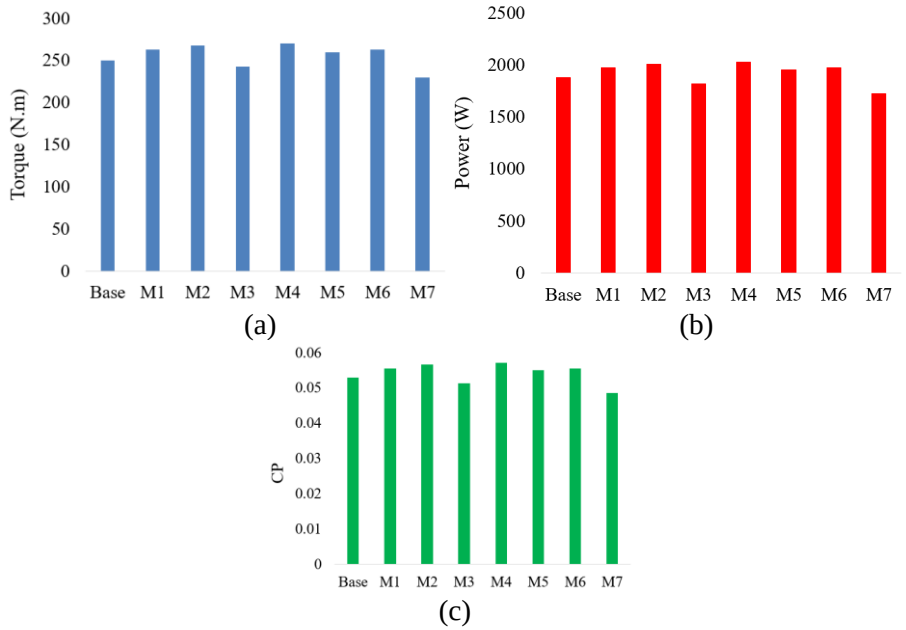

Figure 7. Aerodynamic Performance Results of the Analyzed Blade Models at a Wind Speed of 9 m/s: (a) Rotor Torque, (b) Rotor Power, and (c) Power Coefficient (Cp).

3.4. Aerodynamic Performance Results at a Wind Speed of 11 m/s

The selected wind speed of 11 m/s for this section presents a more challenging operational limit because it shows how increasing aerodynamic loads and decreasing efficiency combined with nonlinear flow effects become more important in critical situations. The blade models underwent wind speed performance testing to show how the new geometric designs will function under conditions where structural and control restrictions take priority over power output needs. The tests used a constant rotor speed of 71.63 rpm to allow direct performance assessment between the different models at their identical operating conditions. The performance data for this section includes aerodynamic torque and output power measurements, which together with the power coefficient, were calculated using standard power computation formulas.

Table 11. Aerodynamic Performance Results at a Wind Speed of 11 m/s.

Model	Rotor torque (N·m)	Rotor power (W)	Power coefficient (Cp)
Base	360.0	2700.4	0.04169
M1	370.8	2781.4	0.04294
M2	374.4	2808.4	0.04336
M3	345.6	2592.4	0.04003
M4	378.0	2835.4	0.04378
M5	367.2	2754.4	0.04253
M6	367.2	2754.4	0.04253
M7	324.0	2430.3	0.03752

Table 12. Percentage Change in The Performance of The Blade Models Relative to the Baseline Configuration at a Wind Speed of 11 m/s.

Model	Torque change (%)	Power change (%)	Cp change (%)
Base	0.0	0.0	0.0
M1	+3.0	+3.0	+3.0
M2	+4.0	+4.0	+4.0
M3	−4.0	−4.0	−4.0
M4	+5.0	+5.0	+5.0
M5	+2.0	+2.0	+2.0
M6	+2.0	+2.0	+2.0
M7	−10.0	−10.0	−10.0

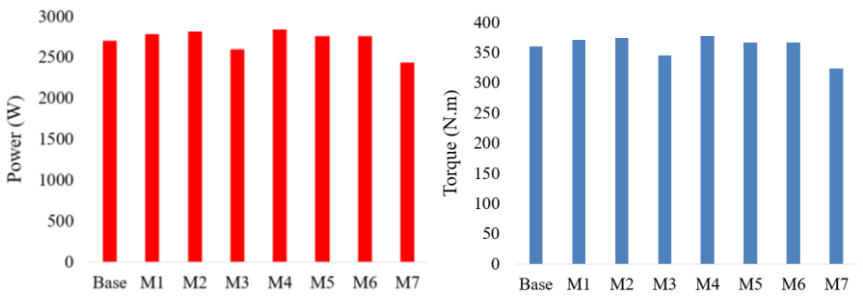

(a) (b)

(c)

Figure 8. Aerodynamic Performance Results of the Analyzed Blade Models at a Wind Speed of 11 m/s: (a) Rotor Torque, (b) Rotor Power, and (c) Power Coefficient (Cp).

The modified blades show less performance improvement at 11 m/s wind speed because their aerodynamic forces and stability limits have increased. The M4 model remains the best performer, offering stable improvement through optimized chord and twist distribution. The M2 model follows with about 4% improvement while M1 provides a modest ~3% gain with stable behavior. The models M5 and M6 deliver minor performance enhancements which reach approximately 2% because their tip-region modifications and root-region reinforcement effects become less significant when the wind speed increases beyond this point. Model M3 shows a 4% performance reduction while model M7 shows a 10% performance reduction because their blade configurations which reduce aerodynamic loads at this wind speed result in decreased power output. The behavior of the system functions as needed for situations that require structural safety and load control to take precedence over achieving the highest possible energy output. The results from this subsection demonstrate that wind speed of 11 m/s does not have any configuration which achieves universal superiority because the optimal blade geometry selection depends on the particular design objectives. Model M4 presents the most effective option to achieve both performance improvements and aerodynamic load management while model M7 functions as a design option which reduces aerodynamic loads through its conservative approach.

4. Conclusion

The section shows the final result of the numerical study which analyzed how wind turbine blades perform in aerodynamic tests. The previous sections show that the NREL Phase VI wind turbine model successfully simulated blade aerodynamic functions through the developed numerical model. The baseline model validation led to the creation of specific changes which included adjusted blade chord length and twist angle and the team studied their performance across different wind speeds. The results demonstrate that aerodynamic behavior changes according to geometric design modifications which depend on the specific flow conditions thus proving that no single blade design performs optimally in all conditions. The numerical data shows clear patterns which researchers can use to create design rules that help with wind turbine blade development and optimization. The results of this study demonstrate that blade designs should clearly match specific operational requirements instead of trying to use common design methods. The baseline blade's aerodynamic torque prediction through numerical methods showed a 10% deviation from NREL Phase VI testing results which occurred at a wind speed of 7m/s. The current numerical framework demonstrates its ability to predict primary aerodynamic loads on horizontal-axis wind turbine blades through this level of agreement with experimental results. The model M1 blade twist distribution was changed to a new specification which maintained the original chord length. The adjustment resulted in improved power output and power coefficient which maintained stable performance throughout the different wind speeds. The results demonstrate that proper control of the local angle of attack along the blade span can enhance aerodynamic efficiency without causing additional aerodynamic loads. The mid-span region of Model M2 which used a longer chord length, brought the greatest power output and power coefficient benefits at moderate wind speeds. The mid-span region serves as the main energy extraction zone which demonstrates high sensitivity to changes in its geometric structure. The M3 blade root, having a shorter chord length, produced lower torque and power at all wind speeds, but reduced blade-hub loads, improving structural integrity. The system of the M4 model used a simultaneous method to modify both the chord length and the twist distribution in order to create equal distribution across the complete system. The system achieved improved torque and power results which included power coefficient results throughout all wind speed testing. The research shows that design methods which use multiple design elements provide better performance stability than design methods which focus on individual design elements or particular design changes. The M6

model brought new features which increased the chord length while it modified the twist design for the root area. The research shows that blade root area functions as a critical element which decreases cut-in wind speed while improving turbine efficiency during low-wind situations. The model M7 implemented geometric changes which aimed to decrease aerodynamic loads. The approach produced power output and power coefficient reductions which confirmed that the configuration could not achieve power output maximization. The configuration serves as a design solution that maintains operational stability during high-wind conditions while enabling load management. The study results demonstrate that different geometric modifications with their specific spanwise positions result in changes to the aerodynamic performance of wind turbine blades. Starting torque reduction and low wind performance decrease mainly result from root region changes whereas mid span changes control power and power coefficient boosting, and tip region plus control changes mainly reduce losses and control loads. Model M4 stands out as the optimal design solution which provides balanced performance to improve wind turbine blade efficiency across different operational scenarios.

Declaration of Competing Interest

The author declares that there are no conflicts of interest regarding the publication of this manuscript.

Funding Information

No funding was received from any financial organization to conduct this research

Author Contributions

Hamid Irhayyim Abdulhussein Imari conceived the research idea, designed the methodology, collected and analyzed the data, conducted the experiments, interpreted the results, and wrote and revised the manuscript. The author approved the final version of the paper.

Acknowledgments

The author acknowledges the Iran University of Science and Technology for its academic support. In addition, the author thanks Al-Furat Al-Awsat Technical University, Technical College of Al-Qadisiyah, Al-Diwaniyah, Iraq, for their valuable assistance.

References

[1] G. M. Joselin Herbert, S. Iniyan, E. Sreevalsan, and S. Rajapandian, ,“A review of wind energy technologies,” Renewable and Sustainable Energy Reviews, vol. 11, no. 6, pp. 1117–1145, Aug. doi: 10.1016/j.rser.2005.08.004.2007.

[2] J. F. Manwell, J. G. McGowan, and A. L. Rogers,, Wind Energy Explained: Theory, Design and Application, 2nd ed. Chichester, U.K.: John Wiley & Sons, doi: 10.1002/9781119994367.2009.

[3] M. O. L. Hansen, Aerodynamics of Wind Turbines, 3rd ed. London, U.K.: Routledge, doi: 10.4324/9781315769981.2015.

[4] T. Burton, D. Sharpe, N. Jenkins, and E. Bossanyi, Wind Energy Handbook, 2nd ed. Chichester, U.K.: John Wiley & Sons, doi: 10.1002/9781119992714.2011.

[5] J. N. Sørensen, ,“Aerodynamic aspects of wind energy conversion,” Annual Review of Fluid Mechanics, vol. 43, pp. 427–448, , doi: 10.1146/annurev-fluid-122109-160801.2011.

[6] N. Khlaifat, A. Altaee, J. Zhou, and Y. Huang, “A review of the key sensitive parameters on the aerodynamic performance of a horizontal wind turbine using computational fluid dynamics modelling,” AIMS Energy, vol. 8, no. 3, pp. 493–524, doi: 10.3934/energy.2020.3.493.2020.

[7] L. Zhou, X. Shen, L. Ma, J. Chen, H. Ouyang, and Z. Du,, “Unsteady aerodynamics of the floating offshore wind turbine due to the trailing vortex induction and airfoil dynamic stall,” Energy, vol. 304, Art. no. 131845, doi: 10.1016/j.energy.2024.131845.2024.

[8] J. Johansen and N. N. Sørensen, ,“Aerofoil characteristics from 3D CFD rotor computations,” Wind Energy, vol. 7, no. 4, pp. 283–294 , doi: 10.1002/we.127.2004.

[9] C. Yiğit and U. Durmaz, “Wind turbine blade design with computational fluid dynamics analysis,” International Journal of Computational and Experimental Science and Engineering (IJCESEN), vol. 3, no. 2, pp. 44–49 .2017.

[10] O. Polat and I. H. Tuncer,(2013), "Aerodynamic shape optimization of wind turbine blades using a parallel genetic algorithm," Procedia Engineering, vol. 61, pp. 28–31, doi: 10.1016/j.proeng.2013.07.149.

[11] M. Caboni, E. Minisci, and A. Riccardi, "Aerodynamic design optimization of wind turbine airfoils under aleatory and epistemic uncertainty," Journal of Physics: Conference Series, vol. 1037, no. 4, Art. no. 042011 , doi: 10.1088/1742-6596/1037/4/042011.2018.

[12] N. E. Boumezbeur and A. Smaili, "An aerodynamic optimization approach for wind turbine blades using proper generalized decomposition," Energies, vol. 18, no. 21, Art. no. 5846, doi: 10.3390/en18215846.2025.

[13] H. Su et al.,,"Optimization of aerodynamic and anti-flutter performance of wind turbine blade airfoils using a hybrid bi-directional cooperative constrained multi-objective evolutionary algorithm," Energy, vol. 333, Art. no. 137337, doi: 10.1016/j.energy.2025.137337.2025.

[14] M. Gao, A. Sun, Y. Zhang, and H. You,, "Application of blades aerodynamic optimization design platform based on the performance of offshore wind turbines," Marine Energy Research, vol. 2, no. 4, Art. no. 10017, doi: 10.70322/mer.2025.10017.2025.

[15] A. A. Firoozi, F. Hejazi, and A. A. Firoozi, ,"Advancing wind energy efficiency: A systematic review of aerodynamic optimization in wind turbine blade design," IDEAS/RePEc .2024.

[16] M. M. Alam, ,"A review of wind turbine blade morphing: Power, vibration, and noise," Fluid Dynamics&Materials Processing, .2025.

[17] A. Najafian and A. Jahangirian,, "Energy optimization through morphing blade design under structural constraints: A case study on the NREL 1.5 MW wind turbine," Science and Technology for Energy Transition, vol. 80, Art. no. 42 doi: 10.2516/stet/2025023.2025

[18] A. E. Faisal et al., "Optimizing the aerodynamic performance of Archimedes spiral wind turbines: A parametric study on blade angle and length at constant radius," Results in Engineering, vol. 27, Art. no. 105785, doi: 10.1016/j.rineng.2025.105785.2025.

[19] J. Deparday, Y. Marikovskiy, I. Abdallah, and S. Barber, "An aerodynamic measurement system to improve the efficiency of wind turbine rotor blades," arXiv preprint, arXiv:2503.08860 , doi: 10.48550/arXiv.2503.08860.2025.

[20] J. M. Catalán, G. Arranz, M. Moriche, M. Guerrero-Hurtado, M. García-Villalba, and O. Flores, ,"Aerodynamic performance and robustness of a nature-inspired concept for a micro-scale wind turbine," arXiv preprint, arXiv:2509.24998 doi: 10.48550/arXiv.2509.24998.2025.

[21] F. Lagos et al, "Recent advances in the analysis of functional and structural polymer composites for wind turbines," Polymers, vol. 17, no. 17, Art. no. 2339, doi: 10.3390/polym17172339.2025.

[22] Z. Zhang, W.-L. Chen, and J. Liu, "Aerodynamic design and analysis for offshore wind turbine blade model," Energy, vol. 330, Art. no. 136659, doi: 10.1016/j.energy.2025.136659.2025

[23] C. Xu, "Relationship between blade shape optimisation and wind energy conversion efficiency," in Proc. 2025 2nd Int. Conf. Electrical Engineering and Intelligent Control (EEIC 2025), Advances in Engineering Research, doi: 10.2991/978-94-6463-864-6_75.2025

[24] A. Nabhani, N. M. Tousi, M. Coma, G. Bugeda, and J. M. Bergada,,"Large-scale horizontal axis wind turbine aerodynamic efficiency optimization using active flow control and synthetic jets," arXiv preprint, arXiv:2407.20746, doi: 10.48550/arXiv.2407.20746.2024

[25] Y. Huang and M. Ge, "Aerodynamic modeling of wind turbine blade considering bending deformation: A modified vortex cylinder model," Physics of Fluids, vol. 37, Art. no. 097109, doi: 10.1063/5.0286547.2025

[26] S. Zhu, H. Tian, H. Zhang, and S. Wang, , "A robust optimization method for wind turbine blade integration based on modal parameterization," Energy Sources, Part A: Recovery, Utilization, and Environmental Effects, vol. 47, no. 2 , doi: 10.1080/15567036.2025.2547080.2025

[27] A. Najafian and A. Jahangirian, "Maximum annual energy production of a 1.5 MW wind turbine using optimum morphing blades at different control management scenarios," Energy Conversion and Management, vol. 326, Art. no. 119429, doi: 10.1016/j.enconman.2024.119429.2025

[28] X. Wang, H. Li, H. Baoyin, S. Han, and C. Bao, , "Aerodynamic optimization of wind turbine blades via surrogate-assisted deep reinforcement learning," Physics of Fluids, vol. 37, Art. no. 047141, doi: 10.1063/5.0256389.2025

[29] W. K. Abbas, M. Abbasalizadeh, and S. Khalilarya, "Design optimization and performance investigation of a micro wind turbine for domestic dwelling used for renewable generation system," Energy Science & Engineering, vol. 13, no. 6, pp. 3386–3409, doi: 10.1002/ese3.70109.2025

[30] H. Seifi Davari, R. M. Botez, M. Seify Davari, and H. Chowdhury, "Enhancing the efficiency of horizontal axis wind turbines through optimization of blade parameters," Journal of Engineering, Art. no. 8574868, doi: 10.1155/2024/8574868.2024

[31] R. Zha et al., ,"A review on performance calculation and design methodologies for horizontal-axis wind turbine blades," Energies, vol. 18, no. 2, Art. no. 435, doi: 10.3390/en18020435.2025.